Journal of Applied Polymer Science

Polysulfone-based composite membranes with functionalized carbon nanotubes show controlled porosity and enhanced electrical conductivity

S. Mangukiya,[1] S. Prajapati,[1] S. Kumar,[2] V. K. Aswal,[3] C. N. Murthy[1]

[1]Applied Chemistry Department, Faculty of Technology and Engineering, P.O. Box 51, Kalabhavan, The M. S. University of Baroda, Vadodara 390001, India

[2]School of Materials Science and Engineering, Gwangju Institute of Science and Technology (GIST), 123 Cheomdangwagi-Ro, Buk-Gu, Gwangju 61005, Korea

[3]Solid State Physics Division, Bhabha Atomic Research Centre, Mumbai 400085, India

Correspondence to: C. N. Murthy (E-mail: chivukula_mn@yahoo.com)

ABSTRACT: Composite membranes of functionalized (–COOH, $–CONH_2$, $–N_3$) carbon nanotubes/polysulfone (CNT/PS) synthesized by the phase-inversion method show unique properties with respect to surface characteristics and the selective separation of metal ions from aqueous solution. Apart from the reduction in the pore size depending on the type of functionalities on the nanotubes, the pure water permeation could reach up to as high as ~600 L m^{-2} h^{-1} (LMH) at reduced pressures and could be due to the functionalized tips of the nanotubes on the membrane surface resulting from the phase inversion process used for the membrane fabrication. The membranes were characterized by small angle neutron scattering (SANS) to confirm the uniform distribution of the nanopores and the surface morphology of the membranes. Results show that rejection of Cu(II) was better than Pb(II) depending on the surface functionality. Interestingly, these membranes also showed enhanced conductivities in the range of 1.0×10^{-2} S cm^{-1}, the conductivity depending on the type of functionality on the nanotubes, thus confirming the presence of functionalized nanotubes tips on the membrane surface. © 2016 Wiley Periodicals, Inc. J. Appl. Polym. Sci. **2016**, *133*, 43778.

KEYWORDS: applications; composites; graphene and fullerenes; membranes; morphology; nanotubes

Received 4 February 2016; accepted 8 April 2016

DOI: 10.1002/app.43778

INTRODUCTION

Polysulfone (PS) was one of the early polymers that was used as membranes and as hollow fibers for desalination[1,2] along with cellulose acetate that was patented by Leob and Sourirajan.[3] These polymers form asymmetric membranes that have a thin skin layer with a porous substructure resulting for the phase inversion process by which these membranes are cast. Carbon nanotubes (CNTs) are being increasingly investigated for their use in polymer matrices for various applications. These include desalination, other separation applications, and even for enhancing the conductivities of polymer matrices. A number of excellent comprehensive reviews are now available[4–6] indicating the intense research activity in this area of composite membranes. From their use in separation technologies, nanotubes have found interesting applications in the design of actuators,[7] in the catalytic membranes,[8] and in the storage devices like fuel cells, batteries, and super capacitors.[9] These nanotubes when incorporated in suitable matrix have been shown to have high electrical conductivity.[10] Polysulfone (PS) is a versatile polymer and has been used even in bio-applications such as hemodialysis, ultrafiltration, and bioreactor technology.[11,12] The thermodynamic, rheological, and the adsorption properties of this polymer have been found to significantly change on its surface modification.[13,14] Therefore, novel nanocomposite membranes containing single-walled carbon nanotubes inside a polysulfone matrix have been reported to show high permeability and diffusiveness for gases like H_2, O_2, CH_4, and CO.[15,16] An increase of up to 67% selectivity between polar and non-polar gases using oxidized nanotubes/polysulfone composite membranes has been reported.[17,18] Due to their tubular nature, nanotubes have been predicted to be useful for selective separation based on size differences of both gases and molecules or ions in the liquid state. It has been shown that pristine single-walled nanotubes as membranes can be used for efficient gas separation[19] and gas

Additional Supporting Information may be found in the online version of this article.

flow was found to be very high for carbon nanotube/polymer nanocomposite membranes.[20] Isophorone diisocyanate-grafted carbon nanotubes incorporated into poly(ether urethane) have shown high water-vapor permeability,[21] whereas CNT/polycarbonate composite membranes have good hydrogen separation properties.[22] For the liquid state, it has been shown that the flow of water through CNTs would be very high due to the very low resistance[23] and large slip lengths. In fact functionalization of the tip of the vertically aligned nanotubes in a polystyrene matrix has been shown to enhance permeation of various liquids, both polar and non-polar.[24] Molecular dynamics simulations on functionalized single-walled nanotubes have shown that presence of charges at the entrance of the pores function as a barrier and helps in prevention of passage of ions thus enhancing the ion rejection, with theoretical predictions being many times better than even the existing separation technologies.[25]

However, it has also been reported that protein fouling behavior of PS composite membranes by bovine serum albumin and ovalbumin has been drastically reduced due to presence of nanotubes,[26] whereas modification on the CNT surface with 5-isocyanato-isophthaloyl chloride enhances the protein adsorption on the membrane.[27] One of the major concerns of membrane based separations is biofouling that leads to reduced water flux and selectivity.[28] Various studies related to flux improvement, pore structure, and size control have been made on polysulfone/CNT composite membranes for application in desalination.[27,29] Due to the increase in hydrophilicity, these composite membranes have been shown to have better antifouling behavior that could be modified by suitable functionalization of the nanotubes.[30] Thin film composite membranes are widely used in sea-water desalination due to their lower internal concentration polarization[31] and taking this into consideration, CNTs have been incorporated both in the polyamide layer[32] and the polysulfone support layer[33] for achieving better flux. PS continues to be a preferred material that has high mechanical strength, acid resistance, and most importantly high water-flux among all membrane materials.[34] Comparing PS and polyethersulfone (PES), it is expected that the compatibility of CNTs and PS will be better than that between CNTs and PES due to the structural differences between PS and PES. We had previously reported the control of porosity by the blending of functionalized MWCNTs with PS to get composite membranes[35] and with SWCNTs to get composite membranes[36] with enhanced removal capacity for various ions separately. A better understanding of the surface structure in terms of pore sizes and pore distribution is still lacking. We now show that the changes in the surface morphology are due to the functionalized nanotubes and correlate it to the possibility of the nanotubes tips being exposed on the membrane surface during the phase inversion process and thus resulting in selectivity of the metal ion separation from a binary mixture and also on its conductivity behavior.

EXPERIMENTAL

Materials

Polysulfone (PS) Udel P-3500 was a gift sample from M/s Solvay Specialty Polymers, Vadodara, India, having molecular weight ~80,000 g mol^{-1}. MWNTs and SWCNTs (diameter: 6–9 nm and 0.7–0.9 nm, respectively) were commercial samples from M/s Sigma Aldrich. Sodium dodecyl sulfate, (SDS, Sigma Aldrich), ethylene diamine (>99%, Sigma Aldrich), and sodium azide (>99%, Sigma Aldrich) were used as received.

Purification and Functionalization of Nanotubes

Many protocols are known for the purification and cleaning of CNTs.[37] However, we used a modified method that was able to remove any amorphous carbon soot and metal catalyst used during the preparation of the CNTs. In our method, about 2.0 g of the raw nanotubes were sonicated with 500 mL of 1% SDS (anionic surfactant) for 2 h. This solution was left undisturbed for ~6 h. The supernatant liquid was decanted and the precipitate was found to be the soot associated with the nanotubes. This supernatant was further centrifuged at 3000 rpm for 15 min and the precipitate rejected. This was repeated 2–3 times and the surfactant associated with the nanotubes was removed by alternate washing with water and brine solution. Subsequently, any metal that may have remained attached to the surface of the CNT's was removed by converting it into soluble metal chlorides by stirring the cleaned nanotubes with 50% HCl solution for 6 h. These nanotubes were subsequently washed and dried. The yield obtained was ~35% of the initial raw CNTs used. Significantly, these cleaned and washed nanotubes are not attracted to the magnetic bar unlike the uncleaned CNTs, which might be containing metals like Fe/Co/Ni that must have been used during their preparation.

Oxidation, Amide, and Azide Functionalization of Carbon Nanotubes

Functionalization of CNTs has been previously reported by our group.[35] In brief, the washed and cleaned CNTs were treated with a 3:1 mixture of concentrated nitric and sulfuric acid (40 mL) for 24 h. These oxidized nanotubes were repeatedly washed with distilled water and then dried under vacuum. Both the single-walled and the multi-walled nanotubes were evaluated for the degree of functionalization in terms of the concentration of the –COOH groups generated on the surface. The titration method was followed where the oxidized nanotubes were added to 0.05 *N* NaOH solution, sonicated for 2 h, stirred for 24 h, and then titrated with 0.05 *N* HCl. The degree of functionalization was estimated to be 6.3 mmol g^{-1} and 4.1 mmol g^{-1} for single-walled and multi-walled nanotubes, respectively. These oxidized nanotubes were further converted to amide and azide functionalized CNTs by treating with thionyl chloride for acylation and further with ethylene diamine for amide functionalization. For azide functionalization, 60 mg of acylated nanotubes were mixed with 5 mg of NaN_3 in *N,N*-dimethyl formamide (DMF) as solvent, and precipitated in toluene. The precipitated product was dried in an oven at 80°C for 4 h. Scheme 1 shows the different steps involved in the functionalization of CNTs. The formation of acid functionalities was confirmed by Raman spectroscopy and is shown in Supporting Information Figure S1 for SWCNTs. The azide functionalization carried out was confirmed from FTIR and shown in Supporting Information Figure S2.

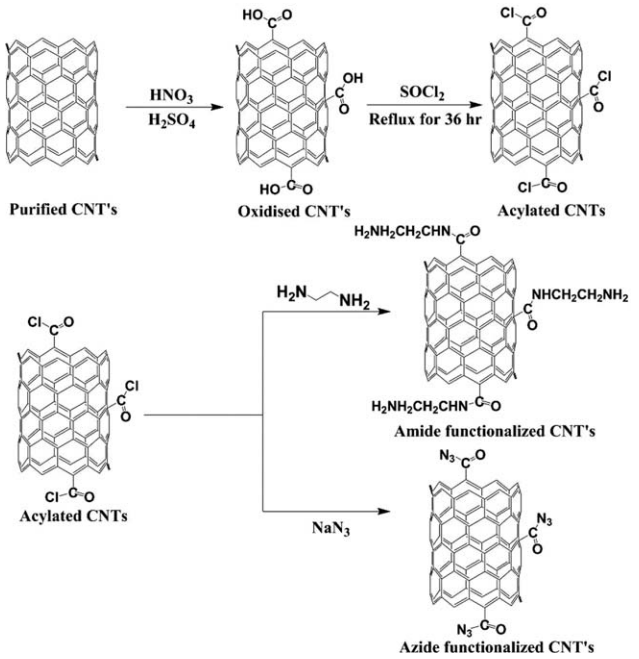

Scheme 1. Schematic of the different steps involved in the functionalization of CNTs.

Blending of CNT's into Polysulfone to Form Nanocomposite Membranes

Initially, polysulfone was dried at 80°C for 24 h under vacuum. *N,N*-dimethyl formamide (DMF) was used as solvent to dissolve the PS. Water with a known concentration of isopropanol was used as coagulation medium during the phase inversion process. An optimized two component dope solution was used, 18% (w/w) polysulfone; 82% (w/w) DMF. Functionalized CNT's at different percentages were added to the polymer solution to form a viscous PS/CNT nanocomposite solution. MWNTs and SWNTs in two different weight percentages (1.0% and 2.0%) were added to the polymer solution, for all the different functionalized CNTs. The solutions were sonicated at 60°C for 12 h to give a black viscous homogeneous solution. Flat sheet membranes were prepared according to the dry/wet phase inversion process, where the polymer solution was poured on the glass plate and stretched into a thin film using a steel casting blade, which rested onto two runners, arranged to form a precise gap of 0.5 mm between the blade and the glass plate. After air-drying for 1 min, the cast membrane was soaked into the coagulating bath, where the solvent/non-solvent exchange takes place and membrane of uniform thickness was formed that within few minutes lifts off from the glass plate. The cast membranes were then thoroughly washed with water, dried at 60°C and then again kept soaked in deionized water for further evaluation.

Flux and Metal Removal Studies

Metal salt solutions were prepared by dissolving the salts in ultrapure water (Elix Millipore) and solutions of 1000 ppm concentration prepared. Stock solutions of lead of 1000 mg L^{-1} concentration were prepared by dissolving 1.598 g of $Pb(NO_3)_2$, in 1 L ultrapure water (Elix, Millipore). Similarly, solution of copper was prepared by dissolving 3.7980 g of $Cu(NO_3)_2$ $3H_2O$ in 1 L water. The solutions were adjusted to 2.6 pH. The permeation tests were conducted at 25°C, effective membrane area was 16.0 cm^2. Pure water flux measurements for the membranes are shown in Table I, where the membranes were compacted at 4.9 bar for 2 h before the flux measurements were carried out.

CHARACTERIZATION

Small Angle Neutron Scattering (SANS)

The small angle neutron scattering (SANS) measurements on the membrane samples over the wave vector range Q ($=4\pi/\lambda \sin\theta$) of 0.015–0.35 $Å^{-1}$ range, where 2θ is the scattering angle and λ is the wavelength of incident neutrons, were taken at 25°C on the SANS diffractometer at the Dhruva reactor, BARC, Mumbai, India. The diffractometer uses a BeO filter as the monochromator. The mean wavelength of the incident neutron beam was 5.2 Å, with a wavelength resolution of approximately 15%. The angular divergence of the incident beam was $\pm 0.5°$ and the beam size at the sample position was 1.5 cm × 1.0 cm. The scattered neutrons were detected using a linear He^3 position-sensitive gas detector. The diffractometer is well suited for the study of a wide variety of systems having characteristic dimensions between 10 and 150 Å. Very few studies are available where neutron scattering is used to study the topology of the membrane surface. The membrane films were cut into small pieces of about 1 cm × 2 cm dimensions and about 4–5 pieces were stacked in an aluminum foil and placed in the path of the beam. The data analysis was done after the data were corrected for the direct beam and background contributions.

Atomic Force Microscopy (AFM)

The atomic force microscopic (AFM) imaging of the selected samples was done on a NTEGRA Aura, NT-MDT make Scanning probe microscope (equipped with the NOVA software) in the semi-contacting mode using an NSG 01 silicone probe. All scans were carried out at room temperature.

Permeation Test

An ultrafiltration test cell was used to evaluate the performance of the CNTs/PS blend membrane. The parameters that were measured are pure water flux and solute rejection of different feed solutions. The solute rejection was calculated using the following equation.

$$\text{Rejection } (\%) = (C_f - C_p)/C_f \times 100 \quad (1)$$

where C_f and C_p are the concentrations of metal ions in the feed solution and permeate, respectively. Both the feed solutions and the filtrate samples were used for quantitative determination of ions using an Atomic Absorption Spectrophotometer (Model: Analytik jena Nova-400) in flame mode/graphite

Table I. Pure Water Flux Measurement Results on the Functionalized Multi-Walled Nanotubes Impregnated Polysulfone at 4.9 Bar Pressure

Code	Type of nanotube	Concentration (%) w/w	Permeate flux (LMH)
M2	Oxidized multi-walled	1.0	203
M3	Amide multi-walled	1.0	210

furnace mode with single beam. The instrument was equipped with 100 mm burner, a cross flow nebulizer 5.0 mL min^{-1} and 1.2 mm slit. All experiments were duplicated under identical conditions.

Conductivity Measurement

Conductivity of the membranes was estimated from the electrochemical impedance spectroscopy (Solatron 1280Z) at room temperature. Before measuring the conductivity all membranes were equilibrated with deionized water for 24 h. The conductivity was calculated from the following equation:

$$\sigma = L/RS \quad (2)$$

where σ is the conductivity (expressed in units of S cm^{-1}), L is the distance between two electrodes used (in cm), R is the resistance of the membrane [in ohms (Ω)], and S is the cross-sectional surface area of the membrane sample (given in cm^2). The cross-sectional surface area was measured for the fully hydrated sample. The impedance of each sample was measured at least five times, to ensure data reproducibility

RESULTS AND DISCUSSION

Characterization of Functionalized Nanotubes

Raman spectroscopy is an effective tool to find the functionalization of nanotubes. The first step in the functionalization of nanotubes is the creation of –COOH groups on the CNTs as mentioned in the Experimental section. The Raman spectra (Supporting Information Figure S1) of the pristine and the acid functionalized SWCNTs gives a clear indication of the creation of the defect structures on the nanotubes edges and the surface due to the acid treatment. The typical I_d/I_g ratio increases due to the increase in the intensity of the I_d band as is expected due to the functionalization i.e. due to the creation of the disordered structures in the SWCNTs. The FT-IR spectra [Supporting Information Figure S2(a)] of oxidized CNT's show a sharp band at 3500 cm^{-1} due to the presence of hydroxyl (–OH) group. Band at 1726 cm^{-1} arises due to the C = O stretching of carboxylic group. Similarly, the strong peak at 1618 cm^{-1} can be assigned to C–O stretching of carboxylic group. Presence of carboxylate anion can also be confirmed by bands present in the range of 1460 cm^{-1}. The spectra of amide functionalized CNT's showed disappearance of the band at 1726 cm^{-1} and appearance of a new band at lower wavenumber (1633 cm^{-1}) due to amide carbonyl stretch. In addition, new bands appeared at 1391 cm^{-1}, corresponding to C–N bond stretching. The azide functionalized nanotubes showed bands at 2142 cm^{-1} and 1566 cm^{-1} [Supporting Information Figure S2(b)] corresponding to the asymmetric stretching and weak symmetric stretching of the azide functional group. As the CNTs were having the required functional groups, therefore were used for blending with polysulfone.

Membrane Casting by Phase-Inversion Process

The details of the different composite membrane samples prepared are given in Table II. The preparation of the composite membranes essentially involved the solvent/non-solvent exchange process when the glass plate coated with the dope solution is immersed in the coagulating bath containing water with isopropanol as a coagulant. Homogenization of the dope solution was critical since, if these solutions are not homogeneous then the film formed would not be uniform and the resulting membrane would have variations in the thickness as well as the porosity. The most easily functionalized part of the nanotubes are the tips that makes them polar and so one of the advantages of the phase inversion process is that, there is a possibility of alignment of the functionalized nanotubes tips towards the surface of the membranes during the process of the phase inversion. This mobility of the nanotubes is dependent on the viscosity of the solution, which was controlled by using 18% solution of the polysulfone. It is known that the process of phase inversion is not only controlled by thermodynamics but also by the kinetics.[38] A higher loading of the polysulfone would give a very high viscosity and was therefore not favored for the casting of the membranes. A lower viscosity was preferred for the phase inversion process, leaving enough time for the nanotubes to realign when the glass substrate is immersed in the water-bath. These membranes retain their asymmetric nature when oxidized or amide functionalized nanotubes are incorporated in the PS. Scanning electron micrographs (SEM) of the cross section of these composite membranes taken after cold fracturing of the membranes confirm this observation. These are shown in Supporting Information Figure S3.

Table II. Sample Details of the Different Nanotubes Impregnated Polysulfone Membranes

Code	Type of nanotube		Concentration (%)
	SWCNT	MWCNT	
M1	—	—	—
M2	—	Oxidized	1.0
M3	—	Amide functional	1.0
M32	—	Amide functional	2.0
M4	—	Azide functional	1.0
M42	—	Azide functional	2.0
S2	Oxidized	—	1.0
S3	Amide functional	—	1.0
S4	Azide functional	—	1.0

Characterization of Composite Membranes

It is known that polysulfone membranes show porous morphology. Addition of MWNTs could help to reduce the pore size, due to small (110–117 nm) diameters of MWNTs and this is what can be seen from the AFM for the membranes with 1% SWCNT and MWCNT in Figure 1. Figure 1(a) is for the oxidized multi-walled CNT impregnated polysulfone (M2) whereas Figure 1(b) is for the oxidized single-walled CNT impregnated polysulfone (Supporting Information Figure S2). AFM pictures clearly show the reduction in the pore diameter from ~600 nm for the multi-walled to ~300 nm for the single-walled nanotubes impregnated CNT. The functionalization of the surface of the nanotubes helps in formation of physical bonds between the polysulfone and the functionalized nanotube and so this influences the formation of the porous structure.

At a similar percent of oxidized nanotubes, it is seen that the single-walled nanotubes give a smoother surface than the

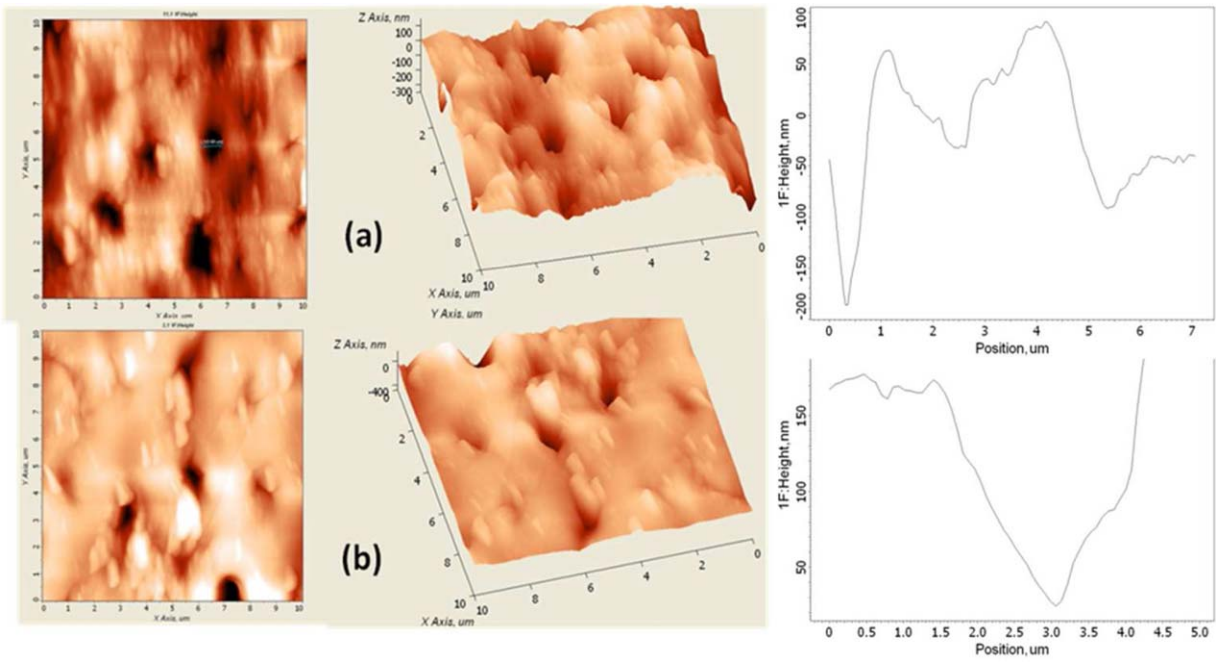

Figure 1. AFM photographs of composite membranes (a) M2 (oxidized) and (b) S2 (oxidized single-walled nanotubes). [Color figure can be viewed in the online issue, which is available at wileyonlinelibrary.com.]

multiwall functionalized nanotubes. This is seen from the force-distance curve on the right side to the Figure 1. In general, the pore sizes are smaller for single-walled functionalized nanotubes.

Small Angle Neutron Scattering

Better structural information about membranes and the pores can be evaluated by SANS experiment and has been used for studying the metallic nanoporous membranes.[39] This technique has been used to determine the nanoparticle dispersion in polyamide membranes[40] and also polydimethyl siloxane based membranes.[41] Since a particle is just defined as a region of different electron density, this can as well be a pore as a solid particle. The basis is that the angular intensity distribution of neutrons scattered by porous materials or hole structures in the range of small angles show that the scattering can be characterized by an exponential correlation function (ξ) in the case of a distribution of holes of random shape and size in a solid. When the correlation function is an exponential, the rule holds that the reciprocal square root of the scattered intensity is a linear function of the square of the scattering angle. The specific surface of the material is determined by the slope of this straight line. Specific surfaces of a number of compositions are calculated from their experimental correlation functions and the pore dimensions calculated based on these scattered intensity. There are two models that are considered: (1) the polydispersed sphere model where the pores are considered to be spherical and surrounded by a matrix material and (2) the random two-phase model, where first phase is the pores and the second phase the surrounding matrix material.

Our data were better fit to the second model where the correlation length is related to the average pore diameter and its distribution and shown in Figure 2. The term $d\Sigma/d\Omega$ on the y-axis, measures the two-dimensional cross-section in the scattering experiment. The correlation lengths and the pore dimensions obtained for our CNT/PS membranes are shown in Table III. Here, it is to be noted that the pore sizes as obtained by the SEM or AFM would be much higher than that obtained by neutron scattering. The advantage of the neutron scattering technique is that one can determine the uniformity of the pores and their distribution on the membrane surface.

As can be seen, there was no change in the correlation length (ζ) as the functionality of the nanotube changed which indicates the uniform distribution of the pores on the surface, however the pore dimension changed with the nature of the nanotube.

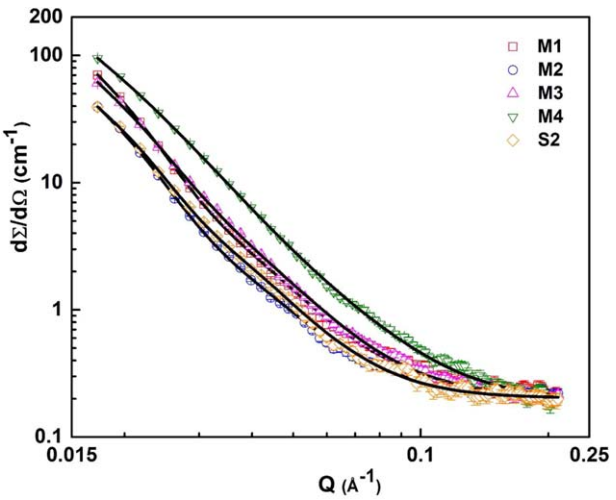

Figure 2. SANS profiles with Debye model fit for (M1) pristine PS, (M2) oxidized MWCNT-1%, (M3) amide MWCNT-1%, (M4) azide MWCNT-1%, and (S2) oxidized SWCNT-1%. [Color figure can be viewed in the online issue, which is available at wileyonlinelibrary.com.]

Table III. SANS Data for Membranes Containing 1% Functionalized Multi-Walled Nanotubes, M1 (Pristine), M2 (Oxidized), M3 (Amide), M4 (Azide), and S2 (Oxidized Single-Walled Nanotubes)

Code	Polydisperse sphere		Debye-Bueche correlation length ξ (nm)
	Mean pore radius R_m (nm)	Polydispersity (σ)	
M1	14.3	0.26	3.8
M2	14.0	0.27	3.9
M3	13.9	0.29	3.9
M4	13.5	0.30	3.9
S2	14.1	0.27	3.9

The mean pore radius reduces from 14.1 nm for the pristine PS membrane, to 13.5 for the MWCNT composite membrane. The effect of the functionalization is clearly seen and there is a smaller pore dimension for the azide functionalized membrane (M4). Comparing the multi-walled and single-walled nanotubes, M2 and S2, there is no change in the pore dimensions, however, between M2 and M4, there is an observable change in the pore dimension thus confirming our contention that the azide fuctionalized nanotube gives smaller pore dimensions.

The permeate flow for 1% oxidized MWCNTs/PS and 1% amide CNTs/PS blend membranes at pressure of 4.9 bar was 203 and 210 LMH, respectively. However, when the membranes were not subjected to any compaction process, the permeation was possible even at lower pressures. When functionalized single-walled nanotubes impregnated polysulfone was used for flux measurement, the pure water flux was measured to be much higher with a value as high as 600 LMH for azide functionalized single-walled nanotubes based membrane subjected to lower pressure of 2.06 bar (Table IV) which was much higher than that obtained for multi-walled nanotube membranes after compaction.

Therefore, the compaction process was done away with and the freshly prepared multi-walled nanotubes based membranes were tested for pure water flux at a low pressure of 1 bar. The results are shown in Table V. As can be seen, these membrane had high flux with the flux increasing with the percentage of functionalized nanotubes, the azide functionalized nanotube membranes giving higher flux than the oxidized nanotubes based membranes.

The possible reason for this increase in the flux could be due to the increased presence of the nanotube tips on the surface during the phase-inversion process and the surface morphology being better as has been found from the SANS studies where the mean pore radius decreases and the polydispersity increases as the tip functionality changes from carboxylate to the azide (Table III).

Table IV. Flux Measurement Results on the Functionalized Single-Walled Nanotubes Impregnated Polysulfone at 2.06 Bar

Code	Type of nanotube	Concentration (%) w/w	Permeate flux (LMH)
S2	Oxidized single-walled	1.0	337
S3	Amide single-walled	1.0	525
S4	Azide single-walled	1.0	600

Table V. Pure Water Flux Measurement Results on the Functionalized Multi-Walled Nanotubes Impregnated Polysulfone at 1 Bar Pressure

Code	Type of nanotube	Concentration (%)	Permeate flux (LMH)
M1	—	—	32
M2	Oxidized multi-walled	1.0	378
M22	Oxidized multi-walled	2.0	500
M4	Azide multi-walled	1.0	446
M42	Azide multi-walled	2.0	545

These observations reflect on the metal removal capacity of the membranes. For the membranes that were subjected to compaction the removal capacities are shown in Table VI. Under these conditions, % rejection of Pb^{2+} for composite membranes containing 1% amide functionalized CNT was 90.1% where as it was 93.1% for Cu^{2+}. The modified MWNTs provide sites for complexation with metal ions which are absent in plain polysulfone membranes. The –COOH due to oxidation of membranes surfaces, –CONH–, and $–CH_2NH_2$ due to amide functionalization and, $–CON_3$ due to azide functionalization show complex formation with metal ions. Apart from these at acidic pH, protons also compete with the heavy metal ions, and thus providing maximum rejection or removal at acidic pH.

Metal removal/rejection studies at the optimized conditions of 2.6 pH and 1 bar pressure were carried out for oxidized, amide functionalized, azide functionalized MWCNT blend membranes in a binary mixture of Pb^{2+} and Cu^{2+} to evaluate the selectivity of the membranes to the removal of the metal ions. Metal ions rejection was found to increase with increase in % weight of CNTs added. Thus for both the metal ions, the removal almost doubled when the oxidized CNT was doubled thus not effecting the selectivity significantly. This may be attributed to the reduced pore size, reduced flow rate, and increased number of active sites on CNTs due to functionalization. The metal removal was found to be more pronounced in case of membranes containing azide (Table VII) functionalized CNTs. The presence of azide groups are expected to have better metal

Table VI. Comparison of Metal Removal Capacity for Multi-Walled Nanotubes at Acidic pH of 2.6 and 4.09 Bar Pressure

Code	Type of nanotube	Concentration (%) w/w	Removal capacity (%)	
			Pb(II)	Cu(II)
M1	None	0.0	10.5	10.1
M2	Oxidized multi-walled	1.0	41.3	79.3
M3	Amide multi-walled	1.0	90.1	93.1
M4	Azide multi-walled	1.0	90.8	93.9

Table VII. Comparison of Metal Removal Capacity for Functionalized Multi-Walled Nanotubes Impregnated Polysulfone Membranes from a Mixture of Pb(II) and Cu(II) at Acidic pH of 2.6 and 1 Bar Pressure

Code	Type of nanotube	Concentration (%) w/w	Removal capacity (%)		Selectivity Pb/Cu
			Pb(II)	Cu(II)	
M2	Oxidized multi-walled	1.0	36.6	40.2	0.91
M22	Oxidized multi-walled	2.0	65.4	79.5	0.82
M4	Azide multi-walled	1.0	22.8	23.3	0.97
M42	Azide multi-walled	2.0	30.1	51.7	0.58

binding capacity as compared to carboxylic group, and thus 90.8% of Pb^{2+} and 93.9% of Cu^{2+} is rejected using an azide CNT/PS blend individually, however in the presence of one other, the rejection actually reduces to 22.8% of Pb^{2+} and 23.3% of Cu^{2+} for azide CNT/PS composite membrane.

This is a surprising result, however this competition for the active sites gets reflected much more clearly when at higher percent of the azide functionalized nanotubes, the rejection for Pb^{2+} increased marginally from 22.8% to 30.1% whereas it almost doubles for Cu^{2+} changing from 23.3% to 51.7% thus effecting the selectivity significantly i.e., the selectivity reduces to half using azide functionalized CNT/PS. It is important to highlight here that these removal capacities were at a significantly low pressure of 1 bar as compared to that at 4.9 bar shown in Table VI.

Conductivity Measurements

The conducting properties of CNTs are well established and it is known that they can have good charge transfer properties.[42,43] Recently it has been shown that functionalized CNTs can be good candidates for efficient charge transfer when incorporated into membranes.[44] It is quite logical that the functionalized nanotubes incorporated into membranes would have conductivities that would be better than those of the matrix. The values of the conductivities are given in Table VIII.

The pristine polysulfone without any nanotubes showed a conductivity of 2.5×10^{-4} S cm^{-1}, whereas the CNT incorporated membranes showed enhanced conductivities with almost a two order increase in the conductivity. The conductivity also depended on the nature of the functionalization, the azide-treated nanotubes giving the highest values. This correlates well with the zeta potential studies of the membranes, which we reported earlier and is shown in Supporting Information Figure S4. As can been seen, the membrane surface attains a different potential depending on the pH. These results also indicate that the functionalized tips of the nanotubes are uniformly distributed on the surface of the membrane.

Table VIII. Conductivities of Functionalized Multi-Walled Nanotubes Measured by the Four-Probe Method

Code	Type of nanotube	Concentration (%) w/w	Conductivity (S cm^{-1})
M1	Polysulfone pristine	-	2.50×10^{-4}
M3	Amide multi-walled	1.0	1.65×10^{-2}
M32	Amide multi-walled	2.0	9.70×10^{-3}
M4	Azide multi-walled	1.0	1.03×10^{-2}
M42	Azide multi-walled	2.0	1.56×10^{-2}

CONCLUSIONS

Our studies indicate that carbon nanotubes (both single-walled and multi-walled) impart excellent rejection properties even at low pressures that open up various opportunities for using these composite membranes as nanofiltration membranes. The surface morphology can be changed by use of suitably functionalized nanotubes that can be aligned due to the phase inversion process used in the membrane fabrication. The uniform dispersion of functionalized nanotubes in the matrix as measured by small angle neutron scattering indicates that thermal stability of these composite membranes will be much higher than the unblended polysulfone. This opens up many high temperature applications for these membranes. Traditional membrane processes involve high pressures that require very high-energy inputs. Thus, for the development of low-pressure processes it requires that the membranes show high pure water flux even at low operating pressures. The membranes reported here show that functionalized nanotubes could be aligned by the phase inversion process used in the casting of the membranes. The permeate flux are significantly high making these composite membranes as potential candidates for pressure retarded processes or even for forward osmosis unlike the present practice of having a polyamide thin layer and a polysulfone support layer. The advantage of these membranes being that the reverse solute transport across the membrane can be restrained due to the presence of the nanotubes, the operating pressures are significantly low, and consequently the fouling of the membrane can be significantly reduced. The percent rejection of metal ions was found to increase with increase in amount of MWNTs. Azide functionalized CNTs showed potential for metal ion selectivity and all the membranes could be potential candidates for proton conduction applications at high temperatures.

ACKNOWLEDGMENTS

This work was funded by UGC-DAE under the grant CRS-M-193, Mumbai India. SM thanks UGC-DAE, India for the fellowship.

REFERENCES

1. Israel, C.; Elias, K.; Smith, J. K. *J. Appl. Polym. Sci.* **1976**, *20*, 2377.
2. Brousse, C.; Chapurlat, R.; Quentin, J. P. *Desalination* **1976**, *18*, 137.
3. Loeb, S.; Sourirajan, S. U.S. Pat 3,133,132. High flow porous membranes for separating water from saline solutions. **1964**.
4. Das, R.; Ali, M. E.; Hamid, S. A.; Ramakrishna, S.; Chowdhury, Z. Z. *Desalination* **2014**, *336*, 97.
5. Goh, P. S.; Ismail, A. F.; Ng, B. C. *Desalination* **2013**, *308*, 2.
6. Kar, S.; Bindal, R. C.; Tewari, P. K. *Nano Today* **2012**, *7*, 385.
7. Fennimore, A. M.; Yuzvinsky, T. D.; Han, W. -Q.; Fuhrer, M. S.; Cumings, J.; Zetti, A. *Nature* **2003**, *424*, 408.
8. Alpatova, A.; Meshref, M.; McPhedran, K. N.; El-Din, M. G. *J. Membr. Sci.* **2015**, *490*, 227.
9. Wang, C.; Waje, M.; Wang, X.; Tang, J. M.; Haddon, R. C.; Yan, Y. *Nano Lett.* **2004**, *4*, 345.
10. Maa, P. C.; Tangb, B. Z.; Kim, J. K. *J. Nanosci. Nanotech.* **2008**, *46*, 1497.
11. Lee, K. W.; Seo, B. K.; Nam, S. T.; Han, M. J. *Desalination* **2003**, *159*, 289.
12. Ahmad, A. L.; Sarif, M.; Ismail, S. *Desalination* **2005**, *179*, 257.
13. Han, M. J.; Nam, S. T. *J. Membr. Sci.* **2002**, *202*, 55.
14. Zhao, Z. P.; Wang, Z.; Wang, S. C. *J. Membr. Sci.* **2003**, *217*, 151.
15. Kim, S.; Chen, L.; Johnson, J. K.; Marand, E. *J. Membr. Sci.* **2007**, *294*, 147.
16. Ahn, J.; Chung, W.-J.; Pinnau, I.; Guiver, M. D. *J. Membr. Sci.* **2008**, *314*, 123.
17. Ge, L.; Zhu, Z.; Rudolph, V. *Sep. Purif. Technol.* **2011**, *78*, 76.
18. Lei, G.; Zhonghua, Z.; Feng, L.; Shaomin, L.; Li, W.; Xuegang, T.; Victor, R. *J. Phys. Chem. C* **2011**, *115*, 6661.
19. Haibin, C.; David, S. S. *J. Mem. Sci.* **2006**, *269*, 152.
20. Kim, S.; Joerg, R.; Jinschek, H. C.; David, S.; Sholl, E. M. *Nano Lett.* **2007**, *7*, 2806.
21. Deng, J.; Zhang, X.; Wang, K.; Zou, H.; Zhang, Q.; Fu, Q. *J. Membr. Sci.* **2007**, *288*, 261.
22. Sharma, A.; Kumar, S.; Tripathi, B.; Singh, M.; Vijay, Y. K. *Int. J. Hydrogen Energy* **2009**, *34*, 3977.
23. Majumder, M.; Chopra, N.; Andrews, R.; Hinds, B. *J. Nature* **2005**, *438*, 44.
24. Majumder, M.; Chopra, N.; Hinds, B. J. *J. Am. Chem. Soc.* **2005**, *127*, 9062.
25. Corry, B. *Energy Environ. Sci.* **2011**, *4*, 751.
26. Celik, E.; Liu, L.; Choi, H. *Water Res.* **2011**, *45*, 5287.
27. Qiu, S.; Wu, L.; Pan, X.; Zhang, L.; Chen, H.; Gao, C. *J. Membr. Sci.* **2009**, *342*, 165.
28. Matin, A.; Khan, Z.; Zaidi, S. M. J.; Boyce, M. C. *Desalination* **2011**, *281*, 1.
29. Choi, J.-H.; Jegal, J.; Kim, W.-N. *J. Membr. Sci.* **2006**, *284*, 406.
30. Yokwana, K.; Gumbi, N.; Adams, F.; Mhlanga, S.; Nxumalo, E.; Mamba, B. *J. Appl. Polym. Sci.* **2015**, *132*, 21, DOI: 10.1002/app.41835
31. Lee, K. P.; Arnot, T. C.; Mattia, D. *J. Membr. Sci.* **2011**, *370*, 1.
32. Lee, H. D.; Kim, H. W.; Cho, Y. H.; Park, H. B. *Small* **2014**, *10*, 2653.
33. Son, M.; Choi, H.-G.; Liu, L.; Celik, E.; Park, H.; Choi, H. *Chem. Engg. J.* **2015**, *266*, 376.
34. Barth, C.; Goncalves, M. C.; Pires, A. T. N.; Roeder, J.; Wolf, B. A. *J. Membr. Sci.* **2000**, *169*, 287.
35. Shah, P.; Murthy, C. N. *J. Membr. Sci.* **2013**, *437*, 90.
36. Gupta, S.; Bhatiya, D.; Murthy, C. N. *Sep. Sci. Tech.* **2015**, *50*, 421.
37. Bonard, J. M.; Stora, T.; Salvetat, J. P.; Maier, F.; Stockli, T.; Duschl, C.; Forro, L.; de Heer, W. A.; Chatelain, A. *Adv. Mater.* **1997**, *9*, 827.
38. Maschado, P. S. T.; Habert, A. C.; Li, C. L. *J. Membr. Sci.* **1999**, *155*, 171.
39. Strunz, P.; Mukherji, D.; Saroun, J.; Keiderling, U.; Rosler, J. *J. Phys. Conf. Ser.* **2010**, *247*, 1.
40. Jadav, G. L.; Aswal, V. K.; Singh, P. S. *J. Colloid Interface. Sci.* **2010**, *351*, 304.
41. Jadav, G. L.; Aswal, V. K.; Singh, P. S. *J. Membr. Sci.* **2015**, *492*, 95.
42. McEuen, P. L. *Nature* **1998**, *393*, 15.
43. Bandaru, P. R. *J. Nanosci. Nanotechnol.* **2007**, *7*, 1239.
44. Gugliuzza, A.; Pingitore, V.; Miriello, D.; Drioli, E. *Phys. Chem. Chem. Phys.* **2015**, *17*, 12919.

SGML and CITI Use Only
DO NOT PRINT